ANALYSIS OF THE PENETRATION CAPABILITY OF VISIBLE SPECTRUM WITH AN ATTENUATION COEFFICIENT THROUGH THE APPARENT OPTICAL PROPERTIES APPROACH IN THE DETERMINATION OF A BATHYMETRY ANALYTICAL MODEL

Kuncoro Teguh Setiawan[1], Gathot Winarso[1], Muhammad Ulin Nuha[2], Maryani Hartuti[1]
Devica Natalia BR Ginting[1], Emi Yati[1], Kholifatul Aziz[1], Fajar Bahari Kusuma[1], Wikanti Asriningrum[1]
[1]Remote Sensing Applications Center-LAPAN
[2]Faculty of Infrastructure and Regional Technology, Institute Teknologi Sumatera
*e-mail: kunteguhs@gmail.com
Received: 6 September 2021; Revised: 1 November 2021; Approved: 29 December 2021

Abstract. The attenuation coefficient (Kd) can be extracted by an apparent optical properties(AOP) approach to determine marine shallow-water habitat bathymetry based on an analytical method. Such a method was employed in the Red Sea by Benny and Dawson in 1983 using Landsat MSS imagery. Therefore, we applied the Benny and Dawson algorithm to extract bathymetry in shallow marine waters off Karimunjawa Island, Jepara, Central Java, Indonesia. We used the SPOT 6 satellite, which has four multispectral bands with a spatial resolution of 6 meters. The results show that three bands of SPOT 6 data (the blue, green, and red bands) can produce bathymetric information up to 30.29, 24.63 and 18.58 meters depth respectively. The determinations of the attenuation coefficients of the three bands are 0.08069, 0.09330, and 0.39641. The overall accuracy of absolute bathymetry of the blue, green, and red bands is 61.12%, 65.73%, and 26.25% respectively, and the kappa coefficients are 0.45, 0.52, and 0.13.

Keywords: *Analytical Method, Benny and Dawson, SPOT 6, Karimunjawa*

1 INTRODUCTION

Bathymetric maps provide ocean depth information that can be used for several purposes, such as shipping, determining suitable areas for ports, and determining coastal cultivation areas. Bathymetric information is needed, especially for shipping safety, because not all Indonesian waters have detailed scale information, especially regarding important ports, amphibious landings, and marine tourism. Bathymetric information is also used as a parameter in tsunami modeling. A suitable tsunami modeling simulation will help in the early warning of a tsunami in a particular area. Updates to bathymetry information are also needed for areas that undergo rapid changes.

The provision and updating of bathymetric information conducted by terrestrial surveys entails very high costs and it takes considerable time to cover a large water area. Bathymetry is usually measured using standard depth measurement tools, such as a multi-beam or single beam echosounders. However, using these tools in shallow waters is time-consuming, especially in Indonesia, an archipelagic country with 77% of the country made up of ocean (Kemenkomarves, 2018). Furthermore, making a depth measurement in shallow water using a multi–beam or single beam echosounder remains tricky because of the operational limitations of the tool, and it can even be dangerous (Kanno, Koibuchi, & Isobe, 2011; Nuha et al., 2019). Therefore, for bathymetric

http://dx.doi.org/10.30536/j.ijreses.2021.v18.a3667

mapping, cheap and safe technology is needed that can cover a large area at one time.

Remote sensing technology has the potential to provide bathymetric information quickly and to cover a wide area. It is known as satellite-derived bathymetry (SDB). Much research has ben conducted on the approach (e.g., Lyzenga, 2006;Kanno et al., 2011, 2012; Arya et al., 2016;Hartuti & Winarso, 2017; Manessaet al., 2014, 2016, 2017; Setiawan et al., 2013, 2014, 2018, 2019, 2020, 2021). However, several problems related to bathymetric information currently exist, including the limited availability of information related to shallow sea waters provided by the relevant agencies. The results of existing SDB have not provided the bathymetric information needed in terms of the ability to penetrate deeply and of accuracy. The results of the bathymetric information from existing SDB modeling are also highly dependent on the satellite imagery used. With higher resolutions, satellite imagery will produce better information, but this is constrained by the costs involved. SDB using the empirical method also has weaknesses, in that it does not consider the attenuation coefficient and requires depth of field data. The empirical method will produce better results if it uses more field data, but it involves high costs and considerable time.

Therefore, it is necessary to develop SDB techniques using analytical methods. SDB with an analytical approach is based on the way waves propagate in water. The formation of this model requires an understanding of the optical properties of water and the atmospheric conditions that affect how light travels. The SDB analytical method considers the diffused attenuation coefficient in the water column and is influenced by water quality, such as chlorophyll-a, total suspended solids (TSS), colored dissolved organic matter (CDOM), temperature, salinity, and conductivity.

The diffused attenuation coefficient is calculated from inherent optical properties (IOP) and apparent optical properties (AOP). IOP is calculated from water quality data measured in the field, while AOP is measured using a TriOS Ramses spectrometer. Mathematically, IOP can be used to derive AOP through the radiative transfer equation. The diversity of conditions in Indonesian waters, such as the level of water quality and atmospheric conditions at each location, will affect the value of the diffused attenuation coefficient. The use of this coefficient will impact the bathymetry estimation generated from satellite imagery.

This paper estimates bathymetry in shallow marine waters using visible wavelengths of SPOT-6 satellite imagery. SPOT 6 was successfully launched on 9th September 2012; its specifications are shown in Table 1-1. This paper also employs an analytical model with the Benny and Dawson algorithm and the attenuation diffusion coefficient using the AOP approach. We focus on Karimunjawa Island, Jepara, Central Java as the study area. The diffused attenuation coefficient was retrieved from the AOP of TriOS Ramses spectral data. We expect that this analytical method could be used for bathymetric mapping in all Indonesian waters using limited in situ data.

Table 1-1 : Specifications of SPOT 6 [https://www.geoimage.com.au/)

Specification	Details
Orbit	Sun-synchronous
Altitude	694 km
Mission Lifetime	10 years
Spatial Resolution	1.5m Panchromatic 6m Multispectral
Accuracy	10 m CE90 at nadir
Spectral Bands	Panchro: 450-745 nm Blue: 450-520 nm Green: 530-590 nm Red: 625-695 nm NIR: 760-890 nm
Stereo Available	Yes – Stereo and Tri-Stereo
Largest Scale	1:5000
Dynamic Range	12 bit
Coverage:	Up to 3m km² per day

2 MATERIALS AND METHODOLOGY

2.1 Location and Data

The research related to the development of the analytical model was conducted on Karimunjawa Island, Jepara, Central Java Province, which is geographically located at coordinates 5°44'18.16"-5°55'22.76"S and 110°24'37.85"-110°31'03.06"E (Figure 2-1).

The satellite image data used for the analytical modeling were from SPOT-6, with a spatial resolution of 6m multispectral, and taken on 6 June 2019. The data processing and analysis were performed at the LAPAN Remote Sensing Utilization Center.

The study also used hydrographic survey data from the waters of Karimunjawa Island. The data were collected during a field survey conducted on September 23rd – 29th, 2019, using measurements from a single beam echosounder, with the coordinates determined by GPS. In situ bathymetry data were used to validate the analytical model, and field surveys were conducted to validate and measure the water quality characteristics. The distribution of the depth of field data collected during the field survey activities is shown in Figure 2-2.

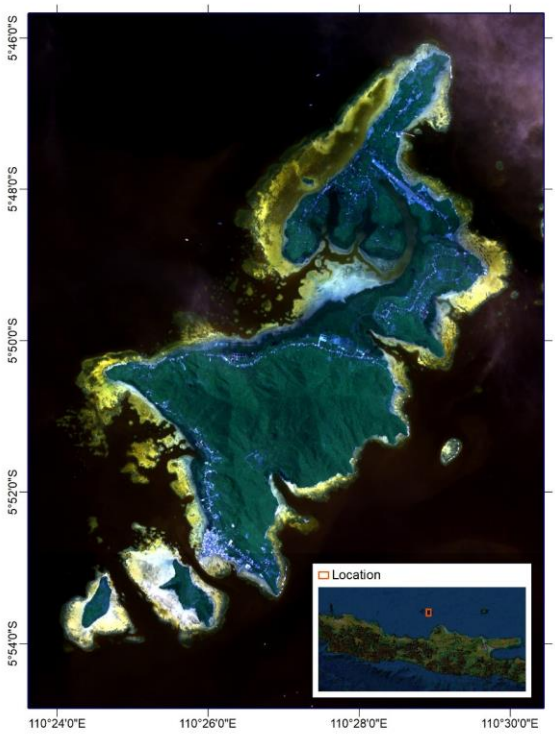

Figure 2-1:Research Location

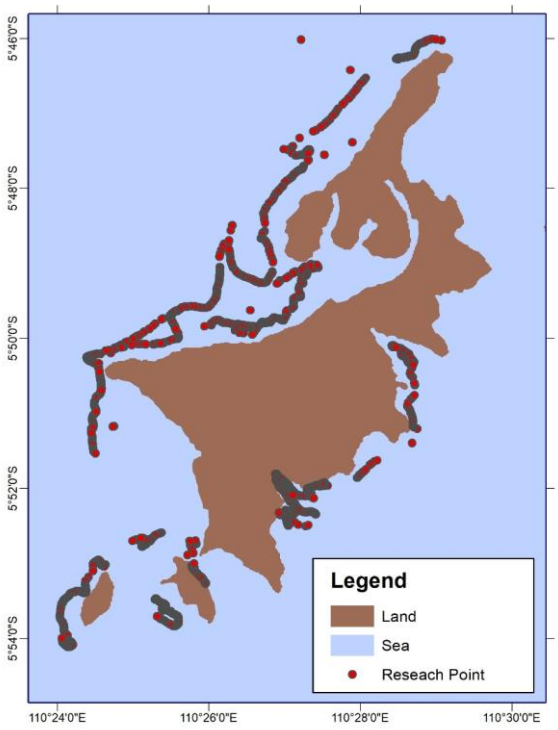

Figure 2-2:In Situ Depth Data Distribution

2.2 Methods

The data processing consisted of image pre-processing, image extraction and accuracy calculations. The pre-processing included atmospheric and radiometric corrections; the atmospheric correction was made using dark object

subtraction, while the radiometric was made using data conversion to reflectance. Homogeneous waters have a K function that depends solely on depth. The diffuse attenuation coefficient of the downwelling Kd (z,λ) is defined by the decreased depth of the ambient downwelling irradiance Ed (z,λ), consisting of photons pointing in all downward directions. The parameters of the AOPs are diffuse attenuation coefficients (Kd), subsurface irradiance reflectance and remote sensing reflectance (Ambarwulan et al., 2013). The difference in the value of Ed (λ) at depth is quantified by equation 1 (Lafon et al., 2002, Lee et al., 2002):

$$Kd(\lambda)=\frac{\ln E_{d1}(\lambda)-\ln E_{d2}(\lambda)}{z1-z2} \quad (2\text{-}1)$$

Kd (λ) is a diffuse spectral attenuation coefficient for the irradiance of the downwelling Ed (λ), which is measured against the difference in depth of z1 and z2. Kd (λ) is one of the apparent optical properties (AOP), which shows the intensity of light absorbed by changes in the water depth (Mobley, 1994; Lee et al., 2005; Simon and Shanmugam, 2016).

The spectrometer measurement data for the calculation of water attenuation used TriOS Ramses. The TriOS Ramses spectrometer consists of three parts, namely ARC VIS (SAM_846A) for measuring upwelling radiance (Lu (λ)); ARC VIS (SAM_846B) for measuring sky radiance (Lsky(λ)); and ACC-2 VIS (SAM_8469) for downwelling irradiance (Ed(λ)) measurement. The configuration of the spectrometer for the measurement of water attenuation is shown in Figure 2-3. Figure 2-3 depicts an illustration of attenuation coefficient measurement.

The Benny and Dawson (1983) concept of wave propagation in water is the basis of the bathymetry value reduction algorithm from the SPOT 6 satellite image extraction in this study. The algorithm for determining the depth of X is as follows:

$$\text{Depth } x=\frac{\log_e(L_x-L_d)-\log_e(L_0-L_d)}{-k(1+\text{cosec}(E'))} \quad (2\text{-}2)$$

where :

Lx = signal recorded by the sensor from water depth x,
Ld = signal recorded by the sensor in deep water (> 30 m),
L_0 = signal recorded by the sensor in shallow water,
k = attenuation coefficient,
E' = angle of reflection of the bottom of the water.

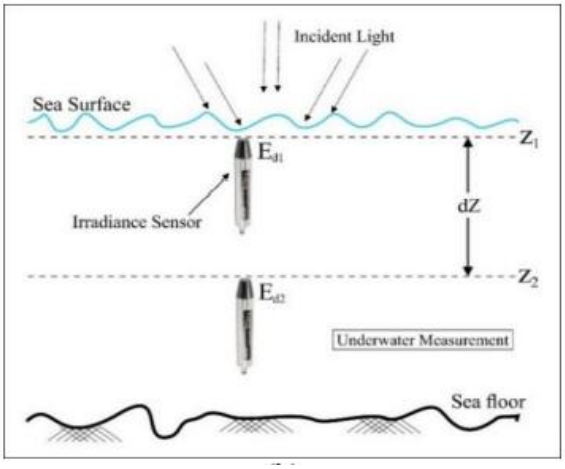

Figure 2-3: Illustration of attenuation coefficient measurement (Prasetyo et al., 2017)

The estimated bathymetry value was determined from the three visible channels, namely the blue, green, and red channels of the SPOT 6 images. The bathymetry values of the results of the three channels were compared with each other to observe the differences, and the accuracy of each extraction of bathymetric information was calculated.

The depth accuracy of each model was calculated using Equations 2-3, 2-4, and 2-5:

$$R^2=1-\sum_i(h_i-\hat{h}_i)^2\Big/\sum_i(h_i-\bar{h})^2 \quad (2\text{-}3)$$

$$ME=\sum_{i=1}^{n}(h_i-\hat{h}_i)\ /n \quad (2\text{-}4)$$

$$RMSE=\left(\sum_{i=1}^{n}(h_i-\hat{h}_i)^2/n\right)^{0.5} \quad (2\text{-}5)$$

where h is the in situ depth measurement; $\hat{h}$ the estimated depth of each model; $\hat{h}$ is the mean in situ depth value; and n the number of input data.

Data accuracy analysis was performed to determine the accuracy of the absolute depth results. Analysis of the accuracy of the data was made using the confusion matrix method. This is a matrix that is arranged to determine the accuracy values of the user accuracy (UA), producer accuracy (PA) and overall accuracy (OA). Mathematically, the three accuracies can be stated as follows (Sampurno and Thoriq, 2016):

$$PA = \frac{x_{ii}}{x_{i+}} \times 100\% \quad (2\text{-}6)$$

$$UA = \frac{x_{ii}}{x_{+i}} \times 100\% \quad (2\text{-}7)$$

$$OA = \frac{\sum_{i=1}^{k} x_{ii}}{N} \times 100\% \quad (2\text{-}8)$$

In addition to calculating the accuracy of the classification results, the matrix will also calculate errors from the image classification results. The matrix has two errors, namely omission error (OE) and commission error (CE). Mathematically, the two errors can be stated as follows (Pamungkas and Jatmiko, 2016):

$$OE = 100\% - PA_x \quad (2\text{-}9)$$

$$CE = 100\% - UA_x \quad (2\text{-}10)$$

where N is the number of depth data in situ used for the observations; x_{ii} is the diagonal value of the i-th row and the i-th column of the confusion matix; x_{+i} is the number of pixels in the i-th column; xi+ is the number of pixels in the i-th row; PA_x is the producer accuracy value in a class and UA_x is the user accuracy value in a class.

In addition to calculating the overall precision using the confusion matrix, the accuracy of the classification results was calculated using kappa analysis. This can be used to compensate for the lack of overall accuracy of the confusion matrix. Calculation of the kappa coefficient is made using the following equation (Djamaluddin et al., 2019):

$$Kappa = \frac{N\sum_{i=1}^{k} x_{ii} - \sum_{i=1}^{k}(x_{i+}x_{+i})}{N^2\sum_{i=1}^{k}(x_{i+}x_{+i})} \quad (2\text{-}11)$$

where N is the total number of all pixels used for the observations; k is the number of lines in the confusion matrix (number of classes); x_{ii} is the diagonal value of the i-th row and i-th column confusion matrix; x_{+i} is the number of pixels in the i-th column, and x_{i+} is the number of pixels in the i-th row.

A value of K ≥ 0.8 indicates outstanding map accuracy; between 0.4 -0.8 corresponds to the medium category; and K ≤ 0.4 indicates the weak category (Congalton, 2001). The flow of the research activity is shown in Figure 2-4.

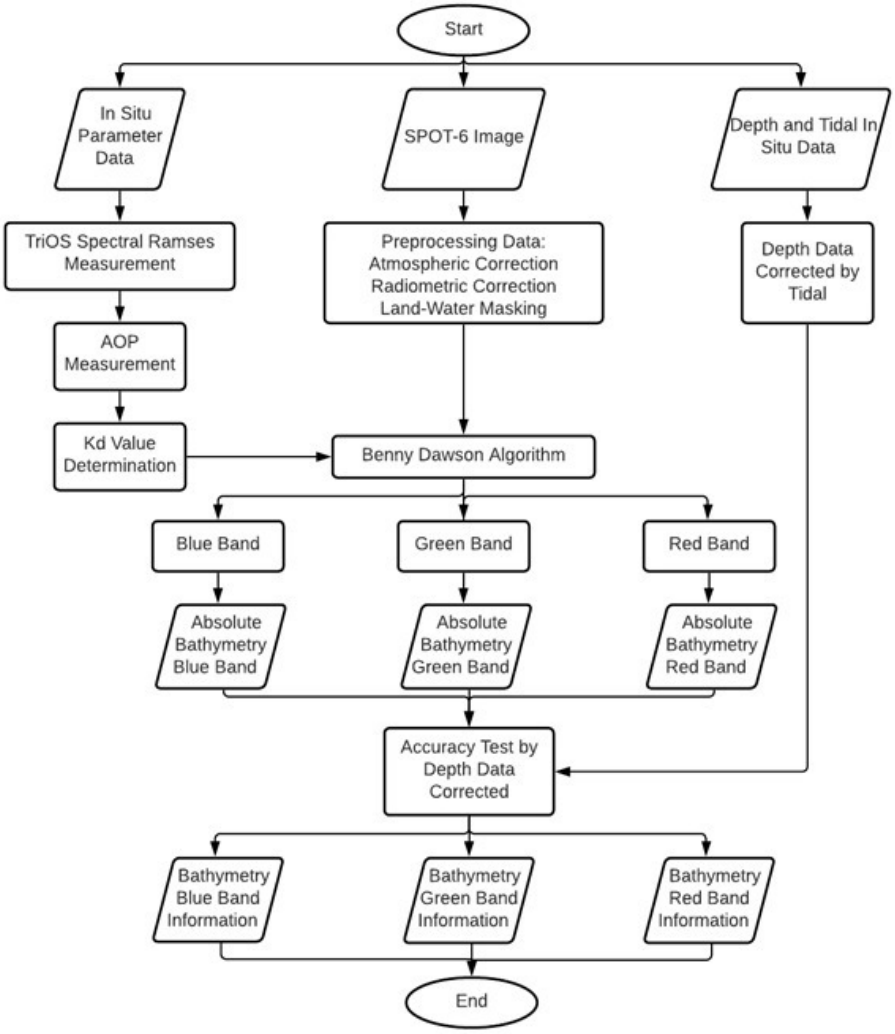

Figure 2-4. Research flow chart

3 RESULTS AND DISCUSSION

The attenuation coefficient and downwelling irradiance of water constituents is a value which defines the property of the water column against light penetration conditions (Gege & Pinnel, 2011). The Ed (λ) used is the average value of the two sets of data obtained. The result of the water attenuation is determined by the value of Ed (λ). Figure 3-1 shows an example of Ed data recording at all the measurement stations for the first data sample at 3m. The Ed data have a regular pattern in the range of 400 to 700 nm, and the wavelengths for the range below 400 nm and above 700 nm have high data variation. This is because the optimal wavelength for penetration in the water column is 400 to 700 nm, the wavelength of visible light (Green et al., 2000; Purkis, 2018).

A high Ed value means a low absorption of light, while a low one indicates high absorption. Ed values in the range of 400-700 nm have different values because of the absorption of energy at different wavelengths (Martin et al., 2012). Attenuation sampling was performed at depths of between 3m and 6m, with a depth difference of 3m. Kd values were calculated for visible light wavelengths (400 – 700 nm) and the wavelengths adjusted to the visible spectrum channel from SPOT 6.

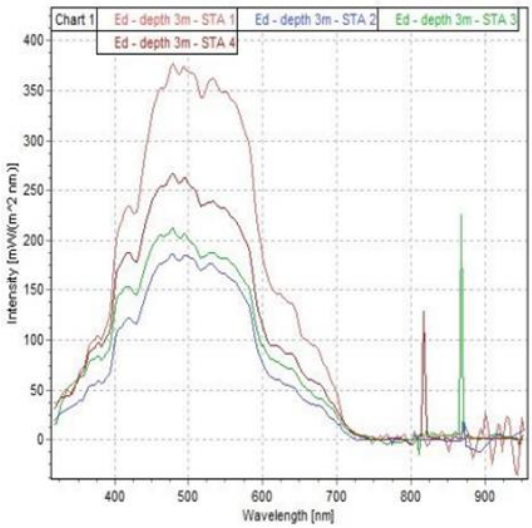

Figure 3-1: Ed data Station 1 plotting (depth = 3 m)

Visible light is the spectrum range of waves that can penetrate the water column. SPOT 6 has three channels for the visible spectrum, consisting of blue (450-525 nm), green (530-590 nm), and red (625-695 nm). Table 3-1 shows the results of the calculation of the average of the Kd values for each wavelength, with the mean calculated for all the data in each wavelength range. The data taken are a range of wavelengths, referring to the method used by Lafon et al. (2002).

Calculations were made for the recorded data obtained by referring to Equation 2-1. Data in Table 3-1 describes a wavelength of 700 nm obtained poor results because at wavelengths above 700 nm, such as NIR, the energy will be entirely absorbed by the water, or will only penetrate a few cm in the water column, meaning there are NAN data and data with negative values. Kd values were calculated for all the wavelength ranges that had values, and are presented in Figure 3-2.

The Kd calculation results in Figure 3-2 show that the visible light wavelength range (400-700 nm) has a reasonably high variation above 600 nm. High variation is shown in the red wavelength range (630-690 nm). This is because the water column will quickly absorb the red waves, so wave attenuation will occur quickly. The blue wavelength (450-510 nm) has a regular pattern of variation in the given results. Based on Saulquin et al.'s (2013) classification, Karimunjawa harbor has clear water types, with an overall average Kd.

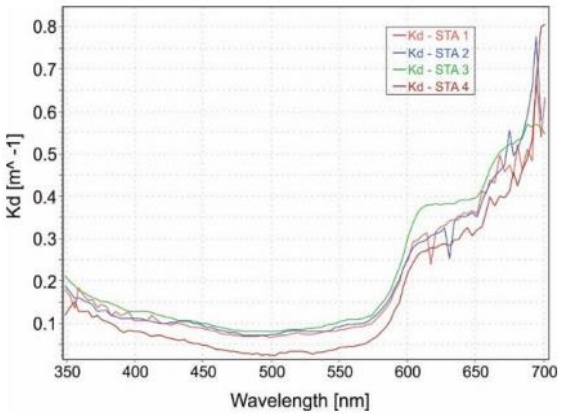

Figure 3-2: Kd Value Plotting

As with the relative depth method, in the absolute depth method, data processing begins with collection of SPOT 6 image data and continues with the data correction process. This process includes atmospheric and radiometric corrections.

Table 3-1: Average of Kd Data Measurements

Station	**Value of Kd m^{-1}**		
	Blue Band	**Green Band**	**Red Band**
Station 1	0.169635	0.189850	0.401958
Station 2	0.020487	0.030857	0.392345
Station 3	0.066190	0.074801	0.438807
Station 4	0.066436	0.077673	0.352547
Average	0.08069	0.09330	039641

The spectral values of the blue, green, and red bands of the SPOT 6 imagery in the waters of Karimunjawa Island were used to extract the bathymetry calculation process to determine absolute depth using the Benny and Dawson algorithm, in line with equation 10. Based on SPOT 6 data dated June 6, 2019, the parameter values for the Benny and Dawson algorithms are listed in Table 3-2.

The depth of penetration (DOP) zone values of each SPOT 6 image band were used from these parameters. The extraction of the DOP zones of the blue, green and red bands yielded depths of up to 30.29 meters, 24.63 meters, and 18.58 meters respectively (Figure 3-3). The extraction results show that the blue band of the SPOT 6 image can penetrate deeper into the water column than the other two bands. The results of the bathymetric information using an analytical model with the Benny and Dawson algorithm are shown in Figure 3-4.

Table 3-2: SPOT 6 Image Parameters

SPOT 6 Image	Blue Band	Green Band	Red Band
Lo	0.10975	0.13625	0.12825
Ld	0.0092	0.0058	0.0046
Kd	0.08069	0.09330	0.39641
Cosec E'		1.8439	

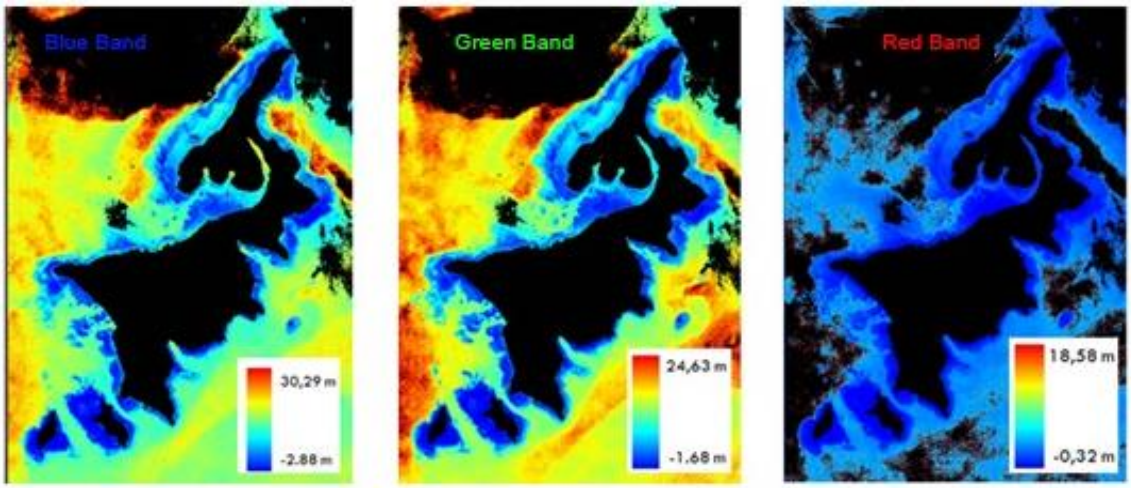

Figure 3-3:Absolute depth of SPOT 6 image

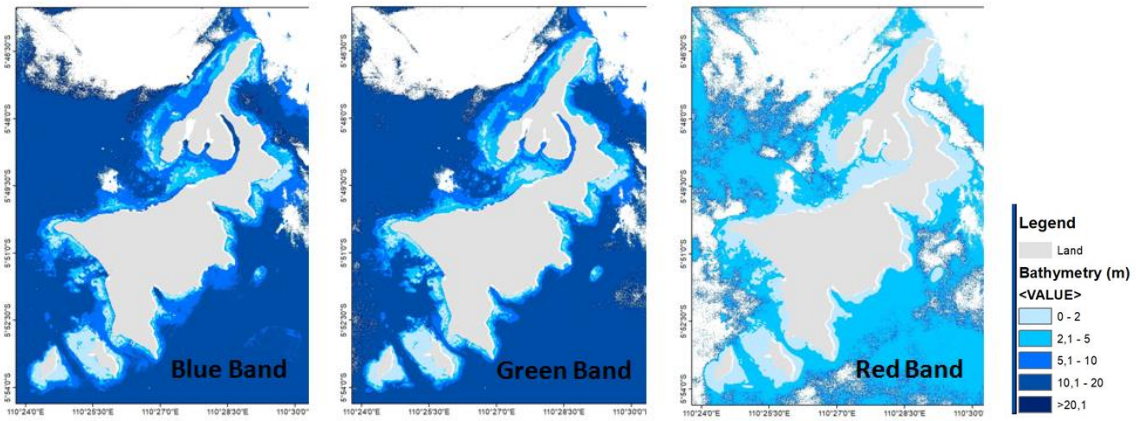

Figures 3-4:Bathymetry Information from SPOT 6 Image

Benny and Dawson's method used in the blue band of SPOT 6 imagery produced accurate results. The calculation of absolute bathymetry accuracy was carried out with 499 points of field data. The accuracy calculations include overall accuracy (OA), user accuracy (UA), producer accuracy (PA), omission error (OE), and commission error (CE). The determination of the accuracy is calculated based on the confusion matrix. The confusion matrix compares the class by the relationship between the field data and the absolute depth result data. The calculation of the accuracy test results can be seen in Tables 3-3, 3-4, and 3-5.

Based on the results of the accuracy test, the overall accuracy value for the absolute bathymetry results from the blue band is 61.12%, with a kappa coefficient value of 0.45, while those from the green band are 65.73%, with a kappa coefficient value of 0.52 and those for the red band 26.25%, with a kappa coefficient value of 0.13. The quality of the bathymetric information related to the two absolute bathymetry results of the blue band and green band is suitable because it has an overall accuracy value above 60%, and the kappa coefficient value is in the range of 0.4 - 0.8, which indicates that it is in the medium category.

The user accuracy (UA) value is the probability that a pixel in the map can correctly represent the class in the field. The absolute bathymetry results from the blue band show that the most significant UA value is in the 5-10 m class, with a value of 72.2%, which has been classified correctly. Although 27.8% of the pixels failed to be mapped according to their class, this was due to the inclusion of an area that should have been removed from a particular class, known as a commission error (CE).

The producer accuracy (PA) value is the probability that all field data are correctly classed. The PA calculation of the absolute bathymetry results from the green band resulted in the 0-2 m class, with the highest PA value of 88.5%. 11.5% of the pixels that should have fallen into the 0-2 m class were not correctly mapped, with an omission error (OE) or discarded areas that should have been included in the class.

The calculation of user accuracy (UA) of the absolute bathymetry results from the red band provided different information from those from the blue and green bands. For a depth of less than 5 meters, the red band has the highest accuracy. However, for depths greater than 5m, the blue and green bands are more accurate. However, for a depth of more than 20 meters, the accuracy of the three bands is still very lacking. This is shown from the absolute bathymetry results from the red band, which have an accuracy of 26.25%, far below 60%, and with a reasonably small kappa coefficient value of 0.13, well below 0.4.

The absolute bathymetry results from the blue band show that the 0-2 m class has a UA accuracy value of 70%, with 30% not mapped according to the class (commission error). Class 2.1-5 m has an accuracy value of 33.3%; class 5.1-10 m has an accuracy value of 72.2%; class 10.1-20 m has an accuracy value of 70.6%; and class > 20 m has an accuracy value of 0%. The results of the calculation of producer accuracy (PA) show that class 0-2 m is that with the highest PA value, at 87.5%. Meanwhile, 12.5% of pixels that should belong to the 0-2 m class are mapped as another class (omission error).

Table 3-3. Blue Band Accuracy Test Results

In situ (m) / Estimation (m)	0 - 2	2.1 - 5	5.1 - 10	10.1 - 20	>20	Row Total	*User Accuracy* (UA)
0 - 2	49	21	0	0	0	70	70%
2.1 - 5	7	20	39	0	0	66	33.3%
5.1 - 10	0	5	104	33	2	144	72.2%
10.1 - 20	0	0	54	132	1	187	70.6%
> 20	0	0	0	32	0	32	0%
Column Total	56	46	197	197	3	499	
Producer Accuracy (PA)	87.5%	43.5%	52.8%	67%	0%		305
Overall Accuracy (OA)	61.12%						
Kappa	0.45						

Table 3-4. Green Band Accuracy Test Results

In situ (m) / Estimation (m)	0 – 2	2.1 – 5	5.1 – 10	10.1 – 20	> 20	Row Total	*User Accuracy* (UA)
0 – 2	46	24	0	0	0	70	65.7%
2.1 – 5	6	30	30	0	0	66	45.5%
5.1 – 10	0	5	114	25	0	144	79.2%
10.1 – 20	0	0	48	138	1	187	73.8%
> 20	0	0	1	32	0	32	0%
Column Total	52	59	192	195	1	499	
Producer Accuracy (PA)	88.5%	50.9%	59.4%	70.8%	0%		328
Overall Accuracy (OA)	65.73%						
Kappa	0,52						

Table 1-5. Red Band Accuracy Test Results

In situ (m) / Estimation (m)	0 – 2	2.1 – 5	5.1 – 10	10.1 – 20	> 20	Row Total	*User Accuracy* (UA)
0 – 2	68	2	0	0	0	70	97.2%
2.1 – 5	19	47	0	0	0	66	71.2%
5.1 – 10	24	109	6	5	0	144	4.2%
10.1 – 20	44	118	15	10	0	187	5.4%
> 20	10	14	3	5	0	32	0%
Column Total	165	290	24	20	0	499	
Producer Accuracy (PA)	41.2%	16.2%	25%	50%	0%		131
Overall Accuracy (OA)	26.25%						
Amount of Data	0.13						

One of the reasons for the increase in accuracy is the wavelength of the image that penetrates the water column. Visible channels (blue, red, and green) can penetrate water to specific depths, and each channel can penetrate deep into the water, especially the blue channel, which penetrates the deepest. Jupp (1988) states that LANDSAT imagery can determine the water depth: Band 1 can penetrate 25 meters deep, Band 2 can penetrate 15 meters, Band 3 can penetrate 5 meters, and Band 4 can penetrate 0.5 meters.

Setiawan et al. (2021) analysed SPOT 7 satellite imagery in shallow sea waters of Karimunjawa Island, Jepara Regency, Central Java Province, with the semi-analytic method of the Benny and Dawson algorithm (1983), capable of producing bathymetry information to a depth of 11.45 meters, generated from the blue band with the Kd of the water column correction.

Shallow water bathymetry mapping using SPOT-7 satellite imagery has previously been conducted by Arya et al. (2016), yielding a depth value of up to 21 meters in the shallow waters of

Mamuju Belangbelang Bay. Their study used a semi-parametric empirical method. Meanwhile, in Siregar's (2010) research, using QuickBird imagery on Panggang Island, Sribu Islands, a depth of up to 10 meters was obtained using Jupp's empirical model. Likewise, the research results of Manesa et al. (2016) produced a depth of up to 11 meters in the shallow waters of Gili Matra Lombok with Worldview-2 multispectral imagery using the empirical random forest method.

Depth measurement with remote sensing technology can be performed by analysing the spectral values of each channel from satellite imagery. Depth measurement with remote sensing data follows the principle that light is weakened through interaction with the water column, referred to as attenuation, and how far the light penetrates the water depends on its wavelength. Shorter wavelength light penetrates water more deeply than that with longer wavelengths (Hutomo, 2010). This principle is based on the Beer-Lambert Law, which states that the absorbance of sunlight will exponentially increase with the increasing concentration of water. Beer-Lambert's law explains that the absorbance of light is exponentially increased to the thickness of the media through which the light is transmitted (Bukata et al., 1995).

4 CONCLUSION

Bathymetry modeling with an analytical model using the Benny and Dawson method (1983) gives the result that using blue, green, and red band bathymetry estimation can produce bathymetric information to depths of 30.29, 24.63, and 18.58 meters respectively, with the determination of the attenuation coefficient being 0.08069, 0.09330 and 0.39641.

Calculation of the absolute accuracy of bathymetry information generated from the blue, green, and red bands shows overall accuracy of 61.12%, 65.73%, and 26.25% respectively, with kappa coefficients of 0.45, 0.52, and 0.13.

ACKNOWLEDGEMENTS

The authors would like to thank Insinas 2019 and PUSFATJA, LAPAN, who facilitated the research. We also thank the UGM Geodetic Team for assisting in the data collection process in the field.

AUTHOR CONTRIBUTIONS

KTS is the main contributor. KTS: conceptualization, methodology, data processing, validating, and analysis. GW and DBG: collecting in-situ data, analysis. MUN and MH: data processing. EY and WA: correction of original draft and formal analysis. KA and FBK: writing and editing.

REFERENCES

Ambarwulan, W., Widiatmaka, & Budhiman, S. (2013). Deriving Inherent Optical Properties From Meris Imagery and in Situ Measurement Using Quasi-Analytical Algorithm. *International Journal of Remote Sensing and Earth Sciences (IJReSES), 10*(1), 1–8. doi: 10.30536/j.ijreses.2013.v10.a1835.

Arya A., Winarso G., & Santoso A.I. (2016). Accuracy Assesment of Satellite Derived Bathymetry using Lyzenga Method and its Modification using SPOT 7 Data at the Belangbelang Bay Waters Mamuju. *J Ilmu Geomatika 22*, 9–19.

Benny, A. H., & Dawson, G. J. (1983). Satellite Imagery as an Aid to Bathymetric Charting in the Red Sea. *The Cartographic Journal, 20*(1), page 12.

Bukata R., Jerome J.H., Kondratyev, K.Y, & Pozdnyakov, D.V. (1995). *Optical Properties and Remote Sensing of Inland*

and Coastal Waters. Boca Raton, Fla: CRC Press.

Congalton, R. G. (2001). Accuracy assessment and validation of remotely sensed and other spatial information. *International Journal of Wildland Fire*, *10*(4), 321-328.

Djamaluddin, M., Ramlan, A., & Jayadi, M. (2019). Monitoring changes in rice fields using a geographic information system application (case study of Pallangga District, Gowa Regency). *Jurnal Ecosolum*, *2*(1), 101-114.

Gege, P., & Pinnel, N. (2011) Sources of Variance of Downwelling Irradiance in Water. *Applied Optics*. Vol. 50, Issue 15 pp. 2192-2203 https://doi.org/10.1364/AO.50.002192

Green E., Mumby P., & Edwards A. & Clark, C. (Eds.) (2000).*Remote Sensing Handbook for Tropical Coastal Management* Coastal Management Sourcebooks, 3. Paris: UNESCO.

Hartuti, M., & Winarso, G. (2017). Extraction of satellite derived bathymetry information from Landsat 8 in Jakarta Bay. *Proceedings, Joint Convention Malang, HAGI –IAGI –IAFMI-IATMI.*

Hutomo A. (2010), Quickbird Imagery Application for Bathymetric Mapping and Shallow Water Basin Object Mapping. Case Study: Roast Gobah, Kepulauan Seribu. Bandung.

Jupp, D.L.B. (1988). Background And Extensions To Depth Of Penetration (DOP) Mapping In Shallow Coastal Waters. In: *Proceedings Of The Symposium On Remote Sensing Of The Coastal Zone, Gold Coast, Queensland, Australia*, pp. IV.2.1 – IV.2.19, September 1988.

Kanno, A., Koibuchi, Y., & Isobe, M. (2011). Shallow Water Bathymetry From Multispectral Satellite Images: Extensions Of Lyzenga's Method For Improving Accuracy. *Coastal Engineering Journal, 53*(4), 431–450,.

Kanno, A., & Tanaka, Y. (2012). Modified Lyzenga's Method for Estimating Generalized Coefficients of Satellite-Based Predictor of Shallow Water Depth. *IEEE Geoscience and Remote Sensing Letters, 9*(4), 715-719.

Kemenko Kemaritiman. 10 Agustus 2018. Coordinating Minister for Maritime Affairs launches reference data for Indonesian marine areas. 2018. Jakarta.

Lafon, V., Froidefond, J.M., Lahet, F., & Castaing, P. (2002). SPOT shallow water bathymetry of a moderately turbid tidal inlet based on field measurements. *Remote Sensing of Environment, 81*(1), 136–148. doi: 10.1093/aje/kwx046.

Lee, Z., Du, K. & Arnone, R. (2005). A model for the diffuse attenuation coefficient of downwelling irradiance. *Journal of Geophysical Research, 110*, 1–10. doi: 10.1029/2004JC002275.

Lyzenga, D. R., Malinas, N. P., & Tanis, F. J. (2006). Multispectral bathymetry using a simple physically based algorithm. *IEEE Transactions on Geoscience and Remote Sensing, 44*(8), 2251–2259. doi: 10.1109/TGRS.2006.872909.

Manessa, M.D.M, Kanno, A., Sekine, M., Ampou, E.E., Widagti, N., & As-syakur, A.R. (2014), Shallow-Water Benthic Identification Using Multispectral Satellite Imagery: Investigation on the Effects of Improving Noise Correction Method and Spectral Cover. *Remote Sens. 2014, 6*, 4454-4472.

Manessa, M.D.M., Kanno, A., Sekine, M., Haidar, M., Yamamoto, K., Imai, T., & Higuchi, T. (2016), Satellite-Derived Bathymetry using Random Forest Algorithm and WorldView-2 Imagery. *Journal of Geomatics and Planning, 3*, (2016), 117-126.

Manessa, M.D.M., Haidar, M. Hartuti, M., & Kresnawati, D.K. (2017). Determination of the Best Methodology of Bathymetry Mapping Using SPOT 6 Imagery: A Study of 12 Empirical Algorithms. *International Journal of Remote Sensing and Earth Sciences, 16*(2), 127-136.

Martin, J., Eugenio, F., Marcello, J., Medina, A., Bermejo, J.A. (2012). Atmospheric correction models for high resolution WorldView-2 multispectral imagery: a case study in Canary Islands, Spain. doi: 10.1117/12.974564.

Mobley, C. D. (1994). *Optical Properties of Water. Light and waters: Radiative Transfer in Natural Waters*, page. 60–144. doi: https://doi.org/10.1016/B978012370626-3.00069-7.

Nuha, M.U., Basith, A., Asriningrum, W., Winarso, G., &Setiawan, K.T. (2019). The Correlation of Attenuation Constants with Water Constituents in Karimunjawa Port. *Elipsoida 02*(01) June 2019. *Jurnal Geodesi UNDIP*.

Pamungkas, B., & Jatmiko, R. H. (2016). Utilization of remote sensing imagery and geographic information systems for erosion mapping in the Serang watershed, Kulonprogo Regency. *Jurnal Bumi Indonesia*, *5*(1), 1-10.

Prasetyo, B. A., Siregar, V. P., Agus, S. B., & Asriningrum, W. (2017) In-Situ Measurement Of Diffuse Attenuation Coefficient And Its Relationship With Water Constituent And Depth Estimation Of Shallow Waters By Remote Sensing Technique. *International Journal of Remote Sensing and Earth Sciences (IJReSES), 14*(1), 47–60.

Purkis, S. J. (2018) Remote Sensing Coral Reefs. Reference Module in Earth Systems and Environmental Sciences. *3 ed. Elsevier Inc., page. 1–8*. doi: 10.1016/B978-0-12-409548- 9.10813-9.

Sampurno, R. M., & Thoriq, A. (2016). Land cover classification using Landsat 8 operational land imager (OLI) images in Sumedang Regency. *Jurnal Teknotan*, *10*(2), 61-70.

Saulquin, B., Hamdib, A., Gohinc, F,. Populusc, J,. Mangina, A,. d'Andona, O.F. (2013). Estimation of the diffuse attenuation coefficient KdPAR using MERIS and application to seabed habitat mapping. *Remote Sensing of Environment, 128*, 224–233. doi: 10.1016/j.rse.2012.10.002.

Setiawan, K.T., (2013), *Study of bathymetry Map Using Landsat ETM+ Data, Case Study at Menjangan Island Bali*. Master's Thesis, Post Graduate Program, Udayana University, Indonesia.

Setiawan,K.T., Osawa, T., Nuarsa, W.2014. AplikasiAlgoritma Van Hengel Dan Spitzer Untuk Ekstraksi informasi Batimetri Menggunakan Data Landsat. Prosiding Sinasja. LAPAN.

Setiawan, K.T., Manessa, M.D.M., Winarso, G., Anggraini, N., Giarrastowo, G., Asriningrum, W., Herianto., Rosid, S., & Supardjo, A.H. (2018). Estimasi Batimetri Dari Data Spot 7 Studi Kasus Perairan Gili Matra Nusa Tenggara Barat. *Jurnal Penginderaan Jauh* Vol. 15 No. 2 Desember 2018:hal 69-82. http://dx.doi.org/10.30536/j.pjpdcd.2018.v15.a3008.

Setiawan, K.T., Suwargana, N.,Ginting. D.N.B., Manessa, M.D.M., Anggraini, N.,Adawiah, S. & Supardjo, A.H. (2019). Bathymetry Extraction From Spot 7 Satellite Imagery Using Random Forest Methods. *International Journal of Remote Sensing and Earth Science* Vol. 16 No. 1June2019. http://dx.doi.org/10.30536/j.ijreses.2019.v16.a3085.

Setiawan, K.T., Ginting, D.N.B., Manessa, M.D.M., Surahman, Winarso, G., Anggraini, N. & Supardjo, A.H. (2020). Bathymetry extraction of empirical models using SPOT 7 satellite imagery. *IOP Conf. Series: Earth and Environmental Science*. doi:10.1088/1755-315/500/1/012063.

Setiawan, K.T., Winarso, G., Ginting, D.N.B, Manessa, M.D.M., Anggraini, N., Surahman & Parwaty, E. (2021). Pemanfaatan Metode Semi-Analitik Untuk Penentuan Batimetri Menggunakan Citra Satelit Resolusi

Tinggi. *Jurnal Penginderaan Jauh* Vol. 18. No. 1Juni 2021:hal1-13. http://dx.doi.org/10.30536/j.pjpdcd.2021.v18.a3409.

Shimon, A., & Shanmugam, P. (2016). Estimation of the Spektral Diffuse Attenuation Coeficient of Downwelling Irradiance in Inland and Coast Waters from Hyperspectral Remote Sensing Data: Validation with Experimental Data. *International Journal of Applied Earth Observation and Geoinformation* Volume 49, July 2016, Pages 117-125. https://doi.org/10.1016/j.jag.2016.02.003.

Siregar, V.P., & Selamat, M.B. (2010).Evaluation of Quickbird Image for Gobah Bathymetry Mapping Using Perum Data: Case Study of Gobah Karang Lebar and Panggang Island. *Jurnal Kelautan UNDIP*.